REPORT DOCUMENTATION PAGE

Form Approved
OMB No. 0704-0188

1. REPORT DATE *(DD-MM-YYYY)*	**2. REPORT TYPE**	**3. DATES COVERED** *(From - To)*
20-11-2006	Journal Article	

4. TITLE AND SUBTITLE

Spectral-Product Methods for Electronic Structure Calculations (Preprint)

5a. CONTRACT NUMBER

5b. GRANT NUMBER

5c. PROGRAM ELEMENT NUMBER

6. AUTHOR(S)
P.W. Langhoff (UCSD); J.E. Mills & J.A. Boatz (AFRL/PRSP)

5d. PROJECT NUMBER
23030423

5e. TASK NUMBER

5f. WORK UNIT NUMBER

7. PERFORMING ORGANIZATION NAME(S) AND ADDRESS(ES)

Air Force Research Laboratory (AFMC)
AFRL/PRSP
10 E. Saturn Blvd.
Edwards AFB CA 93524-7680

8. PERFORMING ORGANIZATION REPORT NUMBER

AFRL-PR-ED-JA-2007-003

9. SPONSORING / MONITORING AGENCY NAME(S) AND ADDRESS(ES)

Air Force Research Laboratory (AFMC)
AFRL/PRS
5 Pollux Drive
Edwards AFB CA 93524-70448

10. SPONSOR/MONITOR'S ACRONYM(S)

11. SPONSOR/MONITOR'S NUMBER(S)
AFRL-PR-ED-JA-2007-003

12. DISTRIBUTION / AVAILABILITY STATEMENT

Approved for public release; distribution unlimited (PAS-07-004)

13. SUPPLEMENTARY NOTES
Submitted for publication in Theoretical Chemistry Acc.

14. ABSTRACT

Progress is reported in development, implementation, and application of a spectral method for ab initio studies of the electronic structure of matter. In this approach, antisymmetry restrictions are enforced subsequent to construction of the many-electron Hamiltonian matrix for an atom or molecule in an orthonormal spectral-product basis. The spectral-product approach to molecular electronic structure avoids the repeated evaluations of the one- and two-electron integrals required in construction of polyatomic Hamiltonian matrices in the antisymmetric basis states commonly employed in conventional calculations of adiabatic potential energy surfaces, providing an alternative ab initio formalism potentially suitable for computational applications more generally.

15. SUBJECT TERMS

16. SECURITY CLASSIFICATION OF:			**17. LIMITATION OF ABSTRACT**	**18. NUMBER OF PAGES**	**19a. NAME OF RESPONSIBLE PERSON**
					Dr. Scott Shackelford
a. REPORT	**b. ABSTRACT**	**c. THIS PAGE**	SAR	27	**19b. TELEPHONE NUMBER** *(include area code)*
Unclassified	**Unclassified**	**Unclassified**			N/A

Spectral-Product Methods for Electronic Structure Calculations[†]

- DRAFT -

P.W. Langhoff,[a] R.J. Hinde,[b] J.D. Mills,[c] and J.A. Boatz[c]

[a] San Diego Supercomputer Center and Department of Pharmacology, University of California, 9500 Gilman Drive, La Jolla, CA 92093-0505

[b] Department of Chemistry, University of Tennessee, Knoxville, TN 37996-1600

[c] Air Force Research Laboratory, 10 East Saturn Blvd., Edwards AFB, CA 93524-7680

(20 November 2006)

Author for correspondence:

Peter W. Langhoff
San Diego Supercomputer Center
University of California San Diego
9500 Gilman Drive, MS 0505
La Jolla, CA 92093-0505

(e-mail - langhoff@drifter.sdsc.edu; Fax - 858-822-0861; Phone 858-822-3611)

[†] Work supported in part by grants from the U.S. Air Force Office of Scientific Research.

Abstract

Progress is reported in development, implementation, and application of a spectral method for *ab initio* studies of the electronic structure of matter. In this approach, antisymmetry restrictions are enforced subsequent to construction of the many-electron Hamiltonian matrix for an atom or molecule in an orthonormal spectral-product basis. Transformation to a permutation-symmetry representation obtained from the eigenstates of the aggregate electron antisymmetrizer is seen to enforce the requirements of the Pauli principle, and to eliminate the unphysical (non-Pauli) states spanned by the product representation. Results identical with conventional use of prior antisymmetrization of configurational state functions in variational calculations are obtained in applications to many-electron atoms, providing some degree of confidence in the soundness of the method more generally. In applications to polyatomic molecules, the development is seen to provide certain potential advantages over conventional methods, and, particularly, to accommodate the incorporation of fragment information in the form of Hermitian matrix representatives of atomic and diatomic operators which include the non-local effects of overall electron antisymmetry. Exact atomic-pair representations of polyatomic Hamiltonian matrices are obtained in this way which avoid the ambiguities of semi-empirical fragment-based methods previously described for electronic structure calculations. Illustrative applications to the well-known low-lying doublet states in the H_3 molecule demonstrate that the eigensurfaces of the antisymmetrizer can anticipate the structures of the more familiar energy surfaces, including the seams of intersections common in high-symmetry molecular geometries. The calculated H_3 energy surfaces are found to be in good agreement with corresponding valence-bond results, and in general accord with accurate values obtained employing conventional high-level computational-chemistry procedures. The spectral-product approach to molecular electronic structure avoids the repeated evaluations of the one- and two-electron integrals required in construction of polyatomic Hamiltonian matrices in the antisymmetric basis states commonly employed in conventional calculations of adiabatic potential energy surfaces, providing an alternative *ab initio* formalism potentially suitable for computational applications more generally.

1.0 Introduction

Considerable progress has been reported over the past four decades in *ab initio* studies of the complex (Born-Oppenheimer) potential energy surfaces which describe the ground and low-lying excited electronic states of molecules [1]. The contributions of Professor Mark S. Gordon to this enterprise have been remarkably comprehensive, as typified by his role in the development, wide-spread distribution, and continuing collaborative refinement of the well-known GAMESS suite of computer codes [2]. Accurate *ab initio* methods provided in this and other computational resources for potential energy surfaces commonly entail repeated calculations of large numbers of one-and two-electron integrals over explicitly antisymmetrized basis states in construction of a many-electron Hamiltonian matrix for a range of atomic spatial arrangements, followed by determinations of the energies and associated eigenfunctions of selected electronic states at each atomic arrangement and construction of the expectation values corresponding to physical properties of interest. New methods for these purposes devised in a spirit of continuing collaborative improvements would clearly be welcome, particularly if they could avoid repeated calculations of the individual electronic integrals and related quantities generally required in the construction of potential energy surfaces, or possibly circumvent entirely determinations of total molecular energies (and their associated differencing problems) in favor of calculations of atomic and interaction energies, while still proving applicable to both ground and electronically-excited states on a common basis.

In a contribution to the systematic improvement of standard quantum-chemical methods, an alternative perspective is provided in the present report on enforcement of the antisymmetry requirement on proper atomic and molecular wave functions [3], which requirement is commonly satisfied by the aforementioned prior constraint on the representational basis states employed in variational calculations. In the present approach, rather, Pauli's exclusion principle is ignored at the outset, and antisymmetry is enforced subsequent to construction of the Hamiltonian matrix in a spectral-product representational basis familiar from the theory of long-range interactions [4]. When applied to the electronic structures of atoms, the development is seen to be equivalent to the familiar Slater approach adopt-

ing prior antisymmetry of many-electron configurational states functions [5], providing some degree of confidence in the alternative method more generally. In applications to polyatomic molecules, the approach provides a number of advantages over conventional methods, and, in particular, accommodates the incorporation of *ab initio* atomic and diatomic information in Hamiltonian matrices in a manner which avoids certain difficulties encountered in previously described semi-empirical fragment-based approaches [6,7].

The present method is ultimately based on conventional variational calculations in L^2 representations of many-electron states, guaranteeing its convergence when closure is achieved, in which limit the distinction between use of simple-product and explicitly antisymmetrized aggregate basis states is shown to become inconsequential. As presented here, the theory is applicable to many-electron atoms and to polyatomic molecules which dissociate into neutral species on their lowest-lying potential energy surfaces, but which can otherwise involve arbitrary admixtures of covalent, ionic, van der Waals, and metallic interatomic interactions. Applications of the approach to ionic systems, or to neutral systems which can give rise to ion-pair states in asymptotic separation limits, require only minor, largely self-evident, modifications of the present description.

The atomic spectral-product basis employed in the development is known to span the totally antisymmetric irreducible representation of the aggregate electron symmetric group once and only once, making it suitable for analytical and computational studies of the electronic structures of many-electron systems [8-12]. The matrix representative of the antisymmetrizer constructed in the spectral-product basis is employed in separating the totally antisymmetric and non-totally-antisymmetric (non-Pauli) states spanned by the basis, and in correspondingly isolating the physically significant block of the Hamiltonian matrix by unitary transformation. Hermitian matrix representations of atomic and atomic-pair operators are devised in this way for polyatomic molecules which individually have well-defined asymptotic separation limits, and which need be constructed only once for multiple applications. These attributes of the approach facilitate development of an *ab initio* unitary transformation formalism which provides an exact atomic-pair representation of polyatomic Hamiltonian matrices, including particularly modifications of the

bare atomic-pair interactions due to aggregate electron antisymmetry consequent of their incorporation in the polyatomic system.

The general theory is described in Section 2, where the spectral-product representation of electrons is defined, the unitary transformation formalism for isolation of the physical portion of the Hamiltonian spectrum is described for both atoms and molecules, and the atomic-pair form of the polyatomic Hamiltonian matrix is reported. Illustrative calculations of the familar low-lying doublet electronic states of the H_3 molecule are provided in Section 3, and concluding remarks made in Section 4.

2.0 Theory

The spectral-product approach to the electronic structures of atoms is described in Section 2.1 as an introduction to the formalism, its application to polyatomic molecules is presented in Section 2.2, and the atomic-pair-based implementation of the approach is reported in Section 2.3.

2.1 Spectral-Product Formalism for Atomic Structure

Solutions of the Schrödinger equation [13]

$$\hat{H}(\boldsymbol{r})\boldsymbol{\Psi}(\boldsymbol{r}) = \boldsymbol{\Psi}(\boldsymbol{r}) \cdot \mathbf{E} \tag{1}$$

for an n-electron atom with Hamiltonian operator [14]

$$\hat{H}(\boldsymbol{r}) = \sum_{i=1}^{n} \Big\{ -\frac{\hbar^2}{2m}\nabla_i^2 - \frac{Ze^2}{r_i} + \sum_{j=i+1}^{n} \frac{e^2}{r_{ij}} \Big\} \tag{2}$$

can be constructed employing a formally complete square-integrable (L^2) representation in the form [8]

$$\boldsymbol{\Phi}(\boldsymbol{r}) = \{\boldsymbol{\phi}(\mathbf{1}) \otimes \boldsymbol{\phi}(\mathbf{2}) \otimes \cdots \boldsymbol{\phi}(\boldsymbol{n})\}_O \,. \tag{3}$$

The row vector $\boldsymbol{\phi}(\boldsymbol{i})$ comprises a denumerable finite or infinite basis set of orthonormal one-electron spin-orbitals specified by the usual quantum numbers (n, l, m_l, s, m_s) [14], where $\boldsymbol{i}$ refers to the spin and space coordinates of the i^{th} electron and $\boldsymbol{r} \equiv (\mathbf{1}, \mathbf{2}, \ldots \boldsymbol{n})$ represents collectively the coordinates of all n atomic electrons. The particular choice of

spin-orbitals is irrelvant for the present development, so long as the outer-product ($\otimes$) Hilbert space of Eq. (3) can include a suitable closure in the limit of a complete spectral basis [15]. The subscript "O" in Eq. (3) indicates the adoption of a particular ordering convention for the sequence of product functions in the row vector $\mathbf{\Phi}(\boldsymbol{r})$, the consequences of which convention are indicated when appropriate in the sequel.

The Hamiltonian matrix representative of the operator of Eq. (2) in the basis of Eq. (3),

$$\mathbf{H} \equiv \langle \mathbf{\Phi}(\boldsymbol{r}) | \hat{H}(\boldsymbol{r}) | \mathbf{\Phi}(\boldsymbol{r}) \rangle = \sum_{i=1}^{n} \Big\{ \mathbf{T}^{(i)} + \mathbf{V}^{(i)} + \sum_{j=i+1}^{n} \mathbf{V}^{(i,j)} \Big\}, \tag{4}$$

includes kinetic $\mathbf{T}^{(i)} \equiv \langle \mathbf{\Phi}(\boldsymbol{r}) | - (\hbar^2/2m) \nabla_i^2 | \mathbf{\Phi}(\boldsymbol{r}) \rangle$, potential $\mathbf{V}^{(i)} \equiv \langle \mathbf{\Phi}(\boldsymbol{r}) | Ze^2/r_i | \mathbf{\Phi}(\boldsymbol{r}) \rangle$, and electron-interaction $\mathbf{V}^{(i,j)} \equiv \langle \mathbf{\Phi}(\boldsymbol{r}) | e^2/r_{ij} | \mathbf{\Phi}(\boldsymbol{r}) \rangle$ Hermitian matrix representatives of the corresponding operators. The dimensions of these matrices are determined by that of the many-electron basis of Eq. (3), although only standard one-and two-electron integrals, and their products with the unit matrices expressing the orthonormality of the remaining n-1 and n-2 orbitals, respectively, are required in evaluations of the Hamiltonian matrix of Eq. (4). The specific forms of these matrices are determined by the particular ordering convention adopted in Eq. (3) [8].

The matrix Schrödinger equation [13]

$$\mathbf{H} \cdot \mathbf{U_H} = \mathbf{U_H} \cdot \mathbf{E} \tag{6}$$

provides approximate or exact representations of the row vector of eigenfunctions of Eq. (1) in the form $\mathbf{\Psi}(\boldsymbol{r}) = \mathbf{\Phi}(\boldsymbol{r}) \cdot \mathbf{U_H}$, as well as the diagonal matrix of associated eigenvalues $\mathbf{E}$. The eigenspectrum so obtained includes both physically significant (totally antisymmetric) and unphysical (non-totally antisymmetric or "non-Pauli") solutions, all of which are spanned by the representation of Eq. (3) [9]. Accordingly, this representation, and the corresponding Hamiltonian matrix and Schrödinger equation of Eqs. (4) and (5), can encompass descriptions of the electrons as either Bose-Einstein, Fermi-Dirac, or possibly other forms of identical particles, necessitating some means of distinguishing among these possibilities [3].

The physical and non-Pauli eigenstates obtained from Eqs. (1) to (6) can be separated by constructing a transformed Hamiltonian matrix which has a physical block, a non-Pauli block, and a vanishing off-diagonal block. This separation is accomplished by constructing the eigenstates of the n-electron antisymmetrizer in the representation of Eq. (3) and transforming the Hamiltonian matrix of Eq. (4) to this new representation. The required representation matrix is

$$\mathbf{P_A} \equiv \langle \mathbf{\Phi}(\boldsymbol{r}) | \hat{P}_A | \mathbf{\Phi}(\boldsymbol{r}) \rangle, \tag{7}$$

where the Hermitian antisymmetrizer employed [3],

$$\hat{P}_A \equiv \sum_{p=1}^{n!} (-1)^{\delta_p} \hat{P}_p, \tag{8}$$

is left unnormalized. The matrix of Eq. (7) is found to comprise a series of individual non-zero $n!$-by-$n!$ blocks on the diagonal the elements of which are all either +1 or -1, and a remaining set of vanishing blocks. The dimensions and natures of the non-zero blocks are associated with the presence of all $(n!)$ permutations of electron assignments to each of the corresponding distinct spin-orbital products in the representation of Eq. (3), which circumstance further insures that any finite atomic representation in the form of Eq. (3) provides an invariant subspace such that the operation of the antisymmetrizer is closed in this subspace

$$\hat{P}_A \mathbf{\Phi}(\boldsymbol{r}) = \mathbf{\Phi}(\boldsymbol{r}) \cdot \mathbf{P_A}. \tag{9}$$

As a consequence, the eigenfunctions of the matrix representative of the antisymmetrizer in any such finite space will transform correctly as either totally antisymmetric or non-totally antisymmetric basis states under all electron permutations [3].

The aforementioned eigenvalues and eigenfunctions of the antisymmetrizer are obtained from the unitary transformation matrix $\mathbf{U_P}$ that diagonalizes the matrix of Eq. (7),

$$\mathbf{U_P^\dagger} \cdot \mathbf{P_A} \cdot \mathbf{U_P} = \begin{pmatrix} (n!)\,\mathbf{I}_{pp} & \mathbf{0} \\ \mathbf{0} & \mathbf{0}_{uu} \end{pmatrix}, \tag{10}$$

where the the physical block $(n!)\,\mathbf{I}_{pp}$ contains the non-zero eigenvalues and the unphysical block $\mathbf{0}_{uu}$ vanishes identically. The individual non-zero $n!$-by-$n!$ blocks indicated above are

each diagonalized separately and contribute a single non-vanishing eigenvalue ($n!$) each to the physical block of Eq. (10), with all other eigenvalues zero. The eigenfunctions of the antisymmetrizer take the correspondingly blocked form

$$\mathbf{\Phi_P}(\boldsymbol{r}) \equiv \mathbf{\Phi}(\boldsymbol{r}) \cdot \mathbf{U_P} = \big\{\{\mathbf{\Phi_P}(\boldsymbol{r})\}_p, \{\mathbf{\Phi_P}(\boldsymbol{r})\}_u\big\}, \tag{11}$$

where the physical states satisfy

$$\hat{P}_A\{\mathbf{\Phi_P}(\boldsymbol{r})\}_p = (n!)\,\{\mathbf{\Phi_P}(\boldsymbol{r})\}_p, \tag{12}$$

and the non-Pauli states provide the null result $\hat{P}_A\{\mathbf{\Phi_P}(\boldsymbol{r})\}_p = \mathbf{0}$. It is found that the physical eigenstates of Eqs. (11) and (12) are Slater determinants made up of the configurations of spin-orbitals comprising the representation of Eq. (3), whereas the non-Pauli eigenstates are totally symmetric or are linear combinations of other (degenerate) representations of the n^{th}-degree symmetric group [16].

Equations (7) to (12) indicate that the spectrum of $\hat{P}_A$ acting in the domain of the spectral-product basis of Eq. (3) is that of a compact operator, with zero providing the lower limiting point of the spectrum and the associated states $\{\mathbf{\Phi_P}(\boldsymbol{r} : \boldsymbol{R})\}_u$ corresponding to a point of accumulation, whereas the totally antisymmetric states $\{\mathbf{\Phi_P}(\boldsymbol{r} : \boldsymbol{R})\}_p$ are associated with the upper limiting point $n!$ and correspond to its point spectrum [17].

The unitary matrix of Eq. (10) provides a transformed Hamiltonian matrix in the form

$$\mathbf{H_P} \equiv \mathbf{U_P^\dagger} \cdot \mathbf{H} \cdot \mathbf{U_P} = \begin{pmatrix} \{\mathbf{H_P}\}_{pp} & \mathbf{0} \\ \mathbf{0} & \{\mathbf{H_P}\}_{uu} \end{pmatrix}, \tag{13}$$

where $\{\mathbf{H_P}\}_{pp}$ and $\{\mathbf{H_P}\}_{uu}$ are the physical (pp) and unphysical (uu) blocks which provide the totally antisymmetric and the non-Pauli solutions, respectively, the off-diagonal blocks vanishing identically in accordance with Eq. (9). The physical Hamiltonian matrix of Eq. (13) is identical with that obtained from the Slater determinants constructed by selecting only linearly-independent ordered spin-orbital configurations from the basis of all such products of Eq. (3). Accordingly, the transformation matrix $\mathbf{U_P}$ of Eq. (10) obtained from the matrix representative of the antisymmetrizer of Eq. (7) correctly incorporates the

effects of electron permutation symmetry, in the absence of prior basis-set antisymmetry, in the Hamiltonian matrix of Eq. (4) through the transformation of Eq. (13).

2.2 Spectral-Product Formalism for Polyatomic Molecules

The foregoing introductory development applies with some important differences and modifications to the adiabatic (Born-Oppenheimer) electronic structures of molecules. Specifically, all quantities given in Section 2.1 now depend explicitly upon the spatial arrangement of atoms in the molecule, specified collectively by $\boldsymbol{R} \equiv (\boldsymbol{R}_1, \boldsymbol{R}_2, ...\boldsymbol{R}_n)$, with the coordinates $\boldsymbol{R}_\alpha$ giving the individual atomic positions. In order to follow closely the atomic development of Section 2.1, and to avoid unnecessary notational complexity, the molecular development is presented here for a collection of n one-electron (hydrogen) atoms [9], with generalization to many-electron atoms requiring only minor additional elaboration [18].

The spectral-product representation of Eq. (3) for polyatomic H_n molecules becomes

$$\boldsymbol{\Phi}(\boldsymbol{r} : \boldsymbol{R}) = \Big\{ \boldsymbol{\phi}^{(1)}(\boldsymbol{1}) \otimes \boldsymbol{\phi}^{(2)}(\boldsymbol{2}) \otimes \cdots \boldsymbol{\phi}^{(n)}(\boldsymbol{n}) \Big\}_O , \tag{14}$$

where the indvidual spectral states $\boldsymbol{\phi}^{(\alpha)}(\boldsymbol{i})$ are the one-electron spin-orbital row vectors of Eq. (3), each now centered at the different origins $\boldsymbol{R}_\alpha$, with the coordinates $\boldsymbol{i}$ measured relative to these centers. As in the atomic case [16], the basis of Eq. (14) spans the totally antisymmetric representation of the aggregate n-electron permutation group once and only once in the limit of closure, as well as all other (non-Pauli) representations of the n^{th}-degree symmetric group in this limit [9].

The molecular Hamiltonian operator is [cf., Eq. (2)]

$$\hat{H}(\boldsymbol{r} : \boldsymbol{R}) \equiv \sum_{\alpha=1}^{n} \Big\{ \hat{H}^{(\alpha)}(\boldsymbol{i}) + \sum_{\beta=\alpha+1}^{n} \hat{V}^{(\alpha,\beta)}(\boldsymbol{i}; \boldsymbol{j} : \boldsymbol{R}_{\alpha\beta}) \Big\}$$

$$= \sum_{\alpha=1}^{n} \Big\{ \{ -\frac{\hbar^2}{2m} \nabla_{i\alpha}^2 - \frac{e^2}{r_{i\alpha}} \} + \sum_{\beta=\alpha+1}^{n} \{ \frac{e^2}{R_{\alpha\beta}} - \frac{e^2}{r_{i\beta}} - \frac{e^2}{r_{j\alpha}} + \frac{e^2}{r_{ij}} \} \Big\}, \tag{15}$$

whereas its matrix representative in the basis of Eq. (14) [cf., Eq. (4)],

$$\mathbf{H}(\boldsymbol{R}) \equiv \langle \boldsymbol{\Phi}(\boldsymbol{r} : \boldsymbol{R}) | \hat{H}(\boldsymbol{r} : \boldsymbol{R}) | \boldsymbol{\Phi}(\boldsymbol{r} : \boldsymbol{R}) \rangle = \sum_{\alpha=1}^{n} \Big\{ \mathbf{H}^{(\alpha)} + \sum_{\beta=\alpha+1}^{n} \mathbf{V}^{(\alpha,\beta)}(\boldsymbol{R}_{\alpha\beta}) \Big\}, \tag{16}$$

is seen to include atomic terms $\mathbf{H}^{(\alpha)} \equiv \langle \boldsymbol{\Phi}(\boldsymbol{r} : \boldsymbol{R}) | \hat{H}^{(\alpha)}(\boldsymbol{i}) | \boldsymbol{\Phi}(\boldsymbol{r} : \boldsymbol{R}) \rangle$ and atomic-pair interaction terms $\mathbf{V}^{(\alpha,\beta)}(\boldsymbol{R}_{\alpha\beta}) \equiv \langle \boldsymbol{\Phi}(\boldsymbol{r} : \boldsymbol{R}) | \hat{V}^{(\alpha,\beta)}(\boldsymbol{i};\boldsymbol{j} : \boldsymbol{R}_{\alpha\beta}) | \boldsymbol{\Phi}(\boldsymbol{r} : \boldsymbol{R}) \rangle$ which provide Hermitian matrix representatives of the corresponding atomic and interaction operators in the molecular Hamiltonian operator of Eq. (15). The atomic energy matrix $\mathbf{H}^{(\alpha)}$ is independent of atomic position and includes only diagonal one-electron energies when the orthonormal atomic spin-orbitals $\boldsymbol{\phi}^{(\alpha)}(\boldsymbol{i})$ are chosen to be atomic pseudo-eigenstates, whereas the interaction matrix $\mathbf{V}^{(\alpha,\beta)}(\boldsymbol{R}_{\alpha\beta})$ is generally non-diagonal and depends explicitly upon the vector separation $\boldsymbol{R}_{\alpha\beta}$ of the two indicated atoms, but not upon the individual laboratory-frame positions of the two atoms, nor upon the position vectors of the other $(n-2)$ atoms in the molecule. The particularly simple form of Eq. (16) is largely a consequence of the orthonormality of the spectral-product basis employed in the absence of prior enforcement of overall electron antisymmetry, and the atomic pairwise-additive nature of the interaction terms in the Hamiltonian operator of Eq. (15).

The Hermitian matrix representative of the antisymmetrizer $\hat{P}_A$ constructed in the basis of Eq. (14),

$$\mathbf{P_A}(\boldsymbol{R}) \equiv \langle \boldsymbol{\Phi}(\boldsymbol{r} : \boldsymbol{R}) | \hat{P}_A | \boldsymbol{\Phi}(\boldsymbol{r} : \boldsymbol{R}) \rangle = (n!)^{-1} \langle \hat{P}_A \boldsymbol{\Phi}(\boldsymbol{r} : \boldsymbol{R}) | \hat{P}_A \boldsymbol{\Phi}(\boldsymbol{r} : \boldsymbol{R}) \rangle, \qquad (17)$$

depends explictly on the atomic arrangement $\boldsymbol{R}$, and is seen to be proportional to the metric matrix of the explicitly antisymmetrized product basis [13]. In contrast to the atomic matrix of Eq. (7), the matrix of Eq. (17) is a complicated function of $\boldsymbol{R}$, requiring detailed computational evaluation. Moreover, the operation of the antisymmetrizer is not closed in any finite representation of the form of Eq. (14), and requires a complete spectral representation to achive closure $\hat{P}_A \boldsymbol{\Phi}(\boldsymbol{r}) \rightarrow \boldsymbol{\Phi}(\boldsymbol{r}) \cdot \mathbf{P_A}$ as a limiting process. This circumstance is a consequence of the fact that, in contrast to the situation in the atomic case of Eq. (3), the representation of Eq. (14) does not include explicitly all $n!$ permutations of electron assignments to the spin-orbital product states appearing there, with exchange terms included only implictly in the limit of a complete spin-orbital representation.

Correspondingly, the unitary transformation matrix $\mathbf{U_P}(\boldsymbol{R})$ required to partition the Hamiltonian matrix of Eq. (16) into physical and non-Pauli blocks is obtained in a limit

from the diagonalization [cf., Eq. (10)]

$$\mathbf{U_P}(\boldsymbol{R})^\dagger \cdot \mathbf{P_A}(\boldsymbol{R}) \cdot \mathbf{U_P}(\boldsymbol{R}) = \begin{pmatrix} \{\mathbf{P}_d(\boldsymbol{R})\}_{pp} & \mathbf{0} \\ \mathbf{0} & \{\mathbf{P}_d(\boldsymbol{R})\}_{uu} \end{pmatrix} \rightarrow \begin{pmatrix} (n!)\mathbf{I}_{pp} & \mathbf{0} \\ \mathbf{0} & \mathbf{0} \end{pmatrix}. \qquad (18)$$

Here, the eigenvalues of the matrix $\mathbf{P_A}(\boldsymbol{R})$ are partitioned into an upper diagonal block $\{\mathbf{P}_d(\boldsymbol{R})\}_{pp}$ containing the largest eigenvalues, which tend to the upper limiting point $(n!)$ of the spectrum in the spectral closure limit, and a lower diagonal block $\{\mathbf{P}_d(\boldsymbol{R})\}_{uu}$ of eigenvalues which tend to zero in this limit [10-12]. Similarly, the eigenstates of the antisymmetrizer in this case are obtained as a limit in the form [cf., Eq. (12)]

$$\mathbf{\Phi_P}(\boldsymbol{r} : \boldsymbol{R}) \equiv \mathbf{\Phi}(\boldsymbol{r} : \boldsymbol{R}) \cdot \mathbf{U_P}(\boldsymbol{R}) \rightarrow \big\{\{\mathbf{\Phi_P}(\boldsymbol{r} : \boldsymbol{R})\}_p, \{\mathbf{\Phi_P}(\boldsymbol{r} : \boldsymbol{R})\}_u\big\}, \qquad (19)$$

where $\{\mathbf{\Phi_P}(\boldsymbol{r} : \boldsymbol{R})\}_p$ contains the totally antisymmetric states corresponding to the non-zero eigenvalues of the antisymmetrizer and $\{\mathbf{\Phi_P}(\boldsymbol{r} : \boldsymbol{R})\}_u$ contains the non-Pauli states corresponding to the zero eigenvalues of the antisymmetrizer.

Finally, the matrix $\mathbf{U_P}(\boldsymbol{R})$ of Eq. (18) is employed in constructing the transformed Hamiltonian matrix

$$\mathbf{H_P}(\boldsymbol{R}) \equiv \mathbf{U_P}(\boldsymbol{R})^\dagger \cdot \mathbf{H}(\boldsymbol{R}) \cdot \mathbf{U_P}(\boldsymbol{R}) = \sum_{\alpha=1}^{n} \Big\{ \mathbf{H_P}^{(\alpha)}(\boldsymbol{R}) + \sum_{\beta=\alpha+1}^{n} \mathbf{V_P}^{(\alpha,\beta)}(\boldsymbol{R}) \Big\}$$

$$= \begin{pmatrix} \{\mathbf{H_P}(\boldsymbol{R})\}_{pp} & \{\mathbf{H_P}(\boldsymbol{R})\}_{pu} \\ \{\mathbf{H_P}(\boldsymbol{R})\}_{up} & \{\mathbf{H_P}(\boldsymbol{R})\}_{uu} \end{pmatrix} \rightarrow \begin{pmatrix} \{\mathbf{H_P}(\boldsymbol{R})\}_{pp} & \mathbf{0} \\ \mathbf{0} & \{\mathbf{H_P}(\boldsymbol{R})\}_{uu} \end{pmatrix}, \qquad (20)$$

where $\mathbf{H_P}^{(\alpha)}(\boldsymbol{R})$ and $\mathbf{V_P}^{(\alpha,\beta)}(\boldsymbol{R})$ refer to transformations of the individual atomic and interaction matrices in Eq. (16), $\{\mathbf{H_P}(\boldsymbol{R})\}_{pp}$ and $\{\mathbf{H_P}(\boldsymbol{R})\}_{uu}$ are the physical (pp) and unphysical (uu) blocks of the transformed Hamiltonian matrix which provide the antisymmetric and the non-Pauli solutions, respectively, and the off-diagonal blocks vanish in the limit $(\rightarrow)$ of spectral closure [9-12]. The transformation of Eq. (20) is seen to incorporate the non-local effects of overall electron antisymmetry on the atomic $\mathbf{H}^{(\alpha)} \rightarrow \mathbf{H_P}^{(\alpha)}(\boldsymbol{R})$ and interaction $\mathbf{V}^{(\alpha,\beta)}(\boldsymbol{R}_{\alpha\beta}) \rightarrow \mathbf{V_P}^{(\alpha,\beta)}(\boldsymbol{R})$ matrices, which consequently now depend on the positions of all atoms in the molecule. Nevertheless, the Hermitian atomic and pair-interaction matrices of Eq. (20) individually have appropriate dissociation limits, with the entire Hamiltonian matrix approaching the sum of the individual atomic terms of Eq. (16) in the complete dissociation limit $\boldsymbol{R} \rightarrow \infty$.

2.3 Atomic-Pair Implementation

The particularly simple forms of the atomic and interaction-energy terms appearing in the Hamiltonian matrix of Eq. (16) suggest the possibility of their systematic evaluation in a series of individual atomic and atomic-pair calculations which can be performed once and for all independently of any particular atomic aggregate arrangement. Since atomic and diatomic eigenspectra are generally available from experimental and previous theoretical studies, it is convenient to cast such an approach in the context of calculations of atomic and diatomic eigenstates and energies, which can be critically evaluated by suitable comparisons prior to their incorporation in the spectral-product representation of Eqs. (14) to (20).

To facilitate the introduction of fragment information, the Hamiltonian operator of Eq. (15) and correponding matrix representative of Eq. (16) can be written in the alternative but equivalent forms [6]

$$\hat{H}(\boldsymbol{r}:\boldsymbol{R}) = \sum_{\alpha=1}^{n} \Big\{ \hat{H}^{(\alpha)}(\boldsymbol{i}) + \sum_{\beta=\alpha+1}^{n} \big\{ \hat{H}^{(\alpha,\beta)}(\boldsymbol{i},\boldsymbol{j}:\boldsymbol{R}_{\alpha\beta}) - \hat{H}^{(\alpha)}(\boldsymbol{i}) - \hat{H}^{(\beta)}(\boldsymbol{j}) \big\} \Big\} \tag{21}$$

and

$$\mathbf{H}(\boldsymbol{R}) = \sum_{\alpha=1}^{n} \Big\{ \mathbf{H}^{(\alpha)} + \sum_{\beta=\alpha+1}^{n} \big\{ \mathbf{H}^{(\alpha,\beta)}(\boldsymbol{R}_{\alpha\beta}) - \mathbf{H}^{(\alpha)} - \mathbf{H}^{(\beta)} \big\} \Big\}, \tag{22}$$

where $\hat{H}^{(\alpha,\beta)}(\boldsymbol{i},\boldsymbol{j}:\boldsymbol{R}_{\alpha\beta}) \equiv \hat{H}^{(\alpha)}(\boldsymbol{i}) + \hat{H}^{(\beta)}(\boldsymbol{j}) + \hat{V}^{(\alpha,\beta)}(\boldsymbol{i};\boldsymbol{j}:\boldsymbol{R}_{\alpha\beta})$ is the diatomic Hamiltonian operator for atoms α and β, and $\mathbf{H}^{(\alpha,\beta)}(\boldsymbol{R}_{\alpha\beta}) = \mathbf{H}^{(\alpha)} + \mathbf{H}^{(\beta)} + \mathbf{V}^{(\alpha,\beta)}(\boldsymbol{R}_{\alpha\beta})$ is its corresponding matrix representative in the basis of Eq. (14). These expressions are sufficient to relate calculations on individual atoms and diatomic molecules in the representation of Eq. (14) to the polyatomic Hamiltonian matrix of Eqs. (16) and (20) also constructed in this basis.

The physical block of the aggregate Hamiltonian matrix of Eq. (20) constructed in this manner takes the form [18]

$$\{\mathbf{H}_{\mathbf{P}}(\boldsymbol{R})\}_{pp} = \sum_{\alpha=1}^{n} \Big\{ \{\mathbf{H}_{\mathbf{P}}^{(\alpha)}(\boldsymbol{R})\}_{pp} + \sum_{\beta=\alpha+1}^{n} \big\{ \mathbf{H}_{\mathbf{P}}^{(\alpha,\beta)}(\boldsymbol{R}) - \mathbf{H}_{\mathbf{P}}^{(\alpha)}(\boldsymbol{R}) - \mathbf{H}_{\mathbf{P}}^{(\beta)}(\boldsymbol{R}) \big\}_{pp} \Big\}, \tag{23}$$

where the atomic matrices $\{\mathbf{H}_{\mathbf{P}}^{(\alpha)}(\boldsymbol{R})\}_{pp}$ and $\{\mathbf{H}_{\mathbf{P}}^{(\beta)}(\boldsymbol{R})\}_{pp}$ are defined in connection with Eq. (20) above, and the physical block of the diatomic Hamiltonian matrix is

$$\{\mathbf{H}_{\mathbf{P}}^{(\alpha,\beta)}(\boldsymbol{R})\}_{pp} = \{\mathbf{U}_{\mathbf{P}}^{(\alpha,\beta)}(\boldsymbol{R})\}_{pp}^{\dagger} \cdot \{\mathbf{H}_{\mathbf{P}}^{(\alpha,\beta)}(R_{\alpha\beta})\}_{pp} \cdot \{\mathbf{U}_{\mathbf{P}}^{(\alpha,\beta)}(\boldsymbol{R})\}_{pp}. \tag{24}$$

Evaluation of Eq. (24) requires the transformation matrix

$$\{\mathbf{U}_{\mathbf{P}}^{(\alpha,\beta)}(\boldsymbol{R})\}_{pp} \equiv \{\langle \mathbf{\Phi}_{\mathbf{P}}^{(\alpha,\beta)}(\boldsymbol{r}_d : \boldsymbol{R}) | \mathbf{\Phi}_{\mathbf{P}}(\boldsymbol{r} : \boldsymbol{R}) \rangle\}_{pp}, \tag{25}$$

where $\{\mathbf{\Phi}_{\mathbf{P}}^{(\alpha,\beta)}(\boldsymbol{r}_d : \boldsymbol{R})\}_p$ and $\{\mathbf{\Phi}_{\mathbf{P}}(\boldsymbol{r} : \boldsymbol{R})\}_p$ are the totally antisymmetric orthonormal states of Eq. (19) for the diatomic molecule (α, β) and for the polyatomic molecule of interest, respectively, whereas the diatomic Hamiltonian matrix in Eq. (24) is given by

$$\{\mathbf{H}_{\mathbf{P}}^{(\alpha,\beta)}(R_{\alpha\beta})\}_{pp} = \{\mathbf{U}_{\mathbf{H}}^{(\alpha,\beta)}(R_{\alpha\beta})\}_{pp} \cdot \{\mathbf{E}^{(\alpha,\beta)}(R_{\alpha\beta})\}_{pp} \cdot \{\mathbf{U}_{\mathbf{H}}^{(\alpha,\beta)}(R_{\alpha\beta})\}_{pp}^{\dagger}, \tag{26}$$

where $\{\mathbf{E}^{(\alpha,\beta)}(R_{\alpha\beta})\}_{pp}$ is the diatomic eigenvalue matrix constructed in the representation of Eq. (14) and $\{\mathbf{U}_{\mathbf{H}}^{(\alpha,\beta)}(R_{\alpha\beta})\}_{pp}$ is the unitary matrix which provides the diatomic eigenfunctions in the form $\{\mathbf{\Psi}^{(\alpha,\beta)}(\boldsymbol{r}_d : \boldsymbol{R})\}_p = \{\mathbf{\Phi}_{\mathbf{P}}^{(\alpha,\beta)}(\boldsymbol{r}_d : \boldsymbol{R})\}_p \cdot \{\mathbf{U}_{\mathbf{H}}^{(\alpha,\beta)}(R_{\alpha\beta})\}_{pp}$. The diatomic states are functions of electron coordinates $(\boldsymbol{r}_d)$ in the diatomic frame, as indicated, and all matrices and vectors in Eqs. (23) to (26) have the dimensions of the representation of Eq. (14), although, with the exception of the polyatomic $\mathbf{P}_{\mathbf{A}}(\boldsymbol{R})$ matrix of Eq. (17), their evaluations require only explicitly atomic and diatomic calculations [18].

The diatomic Hamiltonian matrix of Eq. (24) is seen to include modifications of the corresponding bare diatomic energy matrix appearing in Eq. (26) due to the inter-atomic antisymmetry required upon of immersion of the interacting atomic pair in the molecular aggregate, effects which are incorporated in the development through the indicated transformation matrix. Accordingly, Eqs. (23) and (24) can provide an exact representation of the entire polyatomic Hamiltonian matrix, in the limit of closure, in the form of sums of Hermitian atomic and atomic-pair-interaction matrices which can be determined from atomic and diatomic calculations peformed once and for all independently of any particular atomic arrangement.

3.0 Illustrative Computational Applications

Illustrative computational applications are made of the atomic-pair implementation described in the preceeding section in the case of the H_3 molecule employing a minimal $1s^3$ basis [19] and a 12-term Gaussian representation of the $1s$ atomic hydrogen orbital.

This basis provides an orbital energy (-0.4999 au) in good agreement with the correct value, as well as explicitly antisymmetric singlet and triplet molecular hydrogen eigenstates $\{\mathbf{\Psi}^{(\alpha,\beta)}(\boldsymbol{r}_d : \boldsymbol{R})\}_p$ and a ground-state equilibrium interatomic separation ($R_e = 1.642\ a_0$) and total energy (-1.1157 au) in good agreement with the accepted Heitler-London values. Conventional Gaussian-based computational methods are employed in evaluations of all quantities required in this application of the atomic-pair development for H_3 [2].

In Fig. 1 are shown contour plots of the two doublet eigenvalues of the $\mathbf{P_A}(\boldsymbol{R})$ matrix of Eq. (17) obtained in the $1s^3$ H_3 representation for non-symmetric collinear atomic arrangements. The eigenvalue surface of Fig. 1(a) has a maximum near the saddle point ($R_{ab} = R_{ac} = 1.80\ a_0$), decreases rapidly to zero in the limit $R_{ab} = R_{ac} \to 0$, approaches 1 in the three-body break-up limit $R_{ab} = R_{ac} \to \infty$, and goes to 2 in the diatomic limits $R_{ab} \to 0, R_{ac} \to \infty$ and $R_{ab} \to \infty, R_{ac} \to 0$. The vanishing of the eigenvalue of Fig. 1(a) as R_{ab} and $R_{ac} \to 0$, corresponding to formation of an invalid $1s^3$ atomic Li configuration, indicates that the minimal $1s^3$ basis does not support a physically significant H_3 state in this limit. The smaller doublet eigenvalue surface shown in Fig. 1(b) is evidently less structured than that of Fig. 1 (a) and vanishes in both the diatomic and triatomic united-atom limits. The $\mathbf{P_A}(\boldsymbol{R})$-matrix eigenvalue surfaces evidently identify atomic configurations in which improper states arise, provide information complementary to the associated energy surfaces, and can anticipate the presence of crossings in the corresponding potential energy surfaces, as demonstrated in further detail below.

Figure 2 provides constant-energy contour plots of the two lowest-lying doublet energy surfaces in H_3 obtained from Eqs. (23) to (26) in the $1s^3$ representation for the non-symmetric collinear atomic arrangements of Fig. 1. These well-known energy surfaces are presented here to illustrate the extent of agreement obtained with corresponding conventional valence-bond calculations in a $1s^3$ basis [20], and to demonstrate their general accordance with accurate quantum-chemistry calculations [21-24]. Specifically, the calculated saddle-point energy (-1.574 au) of Fig. 2(a) compares well with that obtained from valence-bond calculations (-1.583 au) in the same basis, and the H_3 geometry at the saddle point ($R_{ab} = R_{ac} = 2.18\ a_0$) is in general accord with the accepted position ($R_{ab} = R_{ac}$

= 1.757 a_0) [21-24]. The current calculation places the saddle point approximately 0.0735 au (2.00 eV) below the three-body (H+H+H) breakup energy of -1.50 au, and thus provides approximately 50% of the accepted accurate saddle-point binding energy of 0.1570 au (4.273 eV) relative to this limit [21-24]. The calculated saddle-point energy relative to the two-body break-up energy (H+H_2) provides a 1.14 eV barrier to the exchange reaction which is in accord with the valence-bond calculations (0.876 eV) but is about three times larger than the accepted value of 0.4166 eV [21-24], emphasizing the well-known sensitivity of this energy difference to the computational approximation employed.

The structure of the ground-state energy surface of Fig. 2(a) is evidently complementary to that of the associated $\mathbf{P_A}(\boldsymbol{R})$-matrix eigenvalue surface of Fig. 1(a), with larger values of the $\mathbf{P_A}(\boldsymbol{R})$-matrix eigenvalues corresponding to generally lower energy values. Similarly, the energy surface for the excited doublet state shown in Fig. 2(b) is seen to be monotonically increasing from the three-atom break-up limit as the diatomic and triatomic united-atom limits are approached, in accord with the monotonically decreasing form of the associated $\mathbf{P_A}(\boldsymbol{R})$-matrix eigenvalue surface of Fig. 1(b).

In Fig. 3 are shown comparisons of the first two doublet energies in H_3 with corresponding valence-bond calculations for symmetric collinear ($R_{ab} = R_{ac}$) atomic arrangements. Evidently, the present results for the ground-state energy surface are in good agreement with the $1s^3$ valence-bond calculations which include only covalent structures ($\circ$), and are also in accord with valence-bond results which include all possible ionic configurations ($\bullet$) in the $1s^3$ basis [20]. The first excited doublet state in H_3 is seen to be repulsive, in good agreement with the valence-bond calculations and in qualitative accord with previously reported accurate calculations, although this excited doublet is known to undergo an avoided crossing with a higher-lying state which is not included in the present development [23]. Although the results of Fig. 3 for the ground-state energy surface appear to bound the valence-bond results from above, this is only a happenstance in view of the small basis set employed. Indeed, similar apparent boundedness is not found for the excited doublet state in Fig. 3, although both results are in satisfactory agreement with the valence-bond calculations, the ionic configurations making generally modest contributions to both states.

Figure 4 depicts contour plots of the two largest doublet-state $\mathbf{P_A}(\boldsymbol{R})$-matrix eigenvalues in H_3 for C_{2v} arrangements in which the $R_{ab} = R_{ac}$ separations are co-varied and the apex angle θ is varied from 30 to 180 degrees. A seam of intersection of these two surfaces indicated by the cusps in the contours is evident in the figures at $\theta = 60$ degrees, which corresponds to the familiar degeneracy associated with D_{3h} symmetry [25]. The dashed and solid portions of the contours in the two figures depict the continuous surfaces which pass smoothly through one another at the $\theta = 60$ degrees line of intersection. In panel (a) the higher-value eigensurface (solid lines) is to the right of the 60 degree line and the lower-value eigensurface (dashed lines) to the left of this line of intersection. Correspondingly, panel (b) shows the reversed arrangement, with the lower eigenvalue surface (dashed lines) to the right and the higher (solid lines) to the left of the 60 degree line. The associated energy surfaces obtained from Eqs. (23) to (26) for the ground- and first-excited doublet states of H_3 for C_{2v} atomic arrangements, shown in Fig. 5, similarly depict the expected D_{3h} degeneracy at $\theta = 60$ degrees and the associated surface crossing along the cusps in the contours, complementary to the corresponding seam of intersection anticipated by the $\mathbf{P_A}(\boldsymbol{R})$-matrix eigenvalues of Fig. 4.

In Fig. 6 are shown comparisons of the two lowest-lying doublet energies in H_3 with coresponding valence-bond calculations for the C_{2v} atomic arrangements of Fig. 5 in which R_{ab} and R_{ac} are held fixed at 1.64 a_0 and θ is varied from 20 to 180 degrees. Evidently, the present results are in good agreement with the corresponding $1s^3$ valence-bond calculations which include only covalent structures ($\circ$). By contrast, although the present results are also in accord with valence-bond results which include all possible ionic configurations ($\bullet$) in the $1s^3$ basis [20], the undulation between 120 and 180 degrees evident upon inclusion of such terms in the valence-bond calculations is evidently not present in the $1s^3$ implementation of the atomic-pair formalism. The crossing of the two surfaces when $\theta = 60$ degrees is evident in the figure, and in accord with the valence-bond calculations. As in Fig. 3, the apparent upper bound provided by the present results on the valence-bond calculations in the case of the ground state in Fig. 6 is a happenstance in view of the small basis representation employed, with a similar apparent upper boundedness not present in the case of the excited doublet state.

4.0 Concluding Remarks

The theoretical development reported in Section 2 provides an alternative perspective on electronic structure calculations for atoms and molecules and other forms of matter. Antisymmetry restrictions are enforced subsequent to construction of the many-electron Hamiltonian matrix for an atom or molecule in an orthogonal spectral-product basis. Transformation to a permutation-symmetry representation obtained from the eigenstates of the aggregate electron antisymmetrizer enforces the requirements of the Pauli principle in this approach. In this way, results are obtained in applications to many-electron atoms which are identical with the use of antisymmetrized configurational state functions in variational calculations, providing some degree of confidence in the soundness of the method more generally. In applications to polyatomic molecules, the development accommodates the incorporation of fragment information in the form of Hermitian matrix representatives of atomic and diatomic operators which include the non-local effects of overall electron antisymmetry on the individual atomic and pairwise-atomic interaction terms.

Illustrative computational applications of the development to the H_3 molecule reported in Section 3 employ largely conventional methods of calculations for atoms and diatomic molecules, and can benefit from the available highly-developed methods devised for this purpose. The eigensurfaces of the matrix representative of the electron antisymmetrizer are seen to identify the presence of non-Pauli states in the spectral-product basis employed, to complement the structures of the more familiar energy surfaces, and to anticipate the presence of seams of surface intersections generally associated with high-symmetry molecular geometries. The minimal-basis-set results reported provide energy surfaces in good agreement with corresponding valence-bond calculations, and are in general accord with the results of accurate quantum-chemistry calculations.

The formalism and applications reported here avoid repeated calculations of the one- and two-electron integrals generally required in construction of polyatomic Hamiltonian matrices employing the antisymmetric basis states commonly adopted in calculations of potential energy surfaces. Accordingly, the approach can possibly provide an alternative *ab initio* method suitable for computational applications to polyatomic molecules more generally.

Acknowledgments

The financial support of the Air Force Research Laboratory, the US Air Force Office of Scientific Research, and the American Society of Engineering Education is gratefully acknowledged. We thank Drs. W. Kalliomaa, R. Channell, J.A. Sheehy, M. Fajardo, and G.A. Gallup for encouragement, support, assistance, and advice in various combinations and at various stages of the investigation.

References

[1] M.R. Hoffmann and K.G. Dyall (Eds.) *Low-Lying Potential Energy Surfaces* (ACS Symposium Series 828, Washington, DC, 2002).

[2] M.W. Schmidt, K.K. Baldridge, J.A. Boatz, S.T. Elbert, M.S. Gordon, J.H. Jensen, S. Koseki, N. Matsunaga, K.A. Nguyen, S.J. Su, T.L. Windus, M. Dupuis, and J.A. Montgomery, GAMESS, J. Comput. Chem. **14**, 1347 (1993).

[3] P.A.M. Dirac, *The Principles of Quantum Mechanics* (Oxford University Press, New York, 1958), 4^{th} Edition, Chapter IX.

[4] H. Eisenschitz and F. London, Z. Physik **60**, 491 (1930).

[5] J.C. Slater, Phys. Rev. **34**, 1293 (1929).

[6] W. Moffitt, Proc. Roy. Soc. (Lond.) A**210**, 245 (1951).

[7] F.O. Ellison, J. Am. Chem. Soc. **85**, 3540 (1963).

[8] P.W. Langhoff, J. Phys. Chem. **100**, 2974 (1996).

[9] P.W. Langhoff, R.J. Hinde, J.A. Boatz, and J.A. Sheehy, Chem. Phys. Lett. **358**, 231 (2002).

[10] P.W. Langhoff, J.A. Boatz, R.J. Hinde, and J.A. Sheehy, in *Low-Lying Potential Energy Surface*, M.R. Hoffmann and K.G. Dyall (Eds.) (ACS Symposium Series 828, Washington, DC, 2002), Chapter 10, pp. 221-237.

[11] P.W. Langhoff, J.A. Boatz, R.J. Hinde, and J.A. Sheehy, in *Fundamental World of Quantum Chemistry: A Tribute to the Memory of Per-Olov Löwdin*, Erkki Brändas and Eugene S. Kryachko (Eds.) (Kluwer Academic, Dordrecht, 2004), Volume 3, pp. 97-114.

[12] P.W. Langhoff, J.A. Boatz, R.J. Hinde, J.A. Sheehy, J. Chem. Phys. **121**, 9323 (2004).

[13] R. McWeeny, *Methods of Molecular Quantum Mechanics* (Academic, London, 1989), 2^{nd} Edition.

[14] E.U. Condon and G.H. Shortley, *The Theory of Atomic Spectra* (Unversity Press, Cambridge, 1963).

[15] R. Courant and D. Hilbert, *Methods of Mathematical Physics* (Interscience, New York, 1966), Volume I, Chapter II.

[16] M. Hammermesh, *Group Theory* (Addison-Wesley, Reading, Massacusetts, 1962).

[17] N.I. Akhiezer and I.M. Glazman, *Theory of Linear Operators in Hilbert Space* (Ungar, New York, 1961), Vol. I.

[18] P.W. Langhoff, R.J. Hinde, J.D. Mills, and J.A. Boatz, J. Chem. Phys. (to be published).

[19] J.C. Slater, Phys. Rev. **38**, 1109 (1931).

[20] G.A. Gallup, *Valence Bond Methods: Theory and Applications* (Cambridge University Press, New York, 2002).

[21] P. Siegbahn and B. Liu, J. Chem. Phys. **68**, 2457 (1978).

[22] S.L. Mielke, B.C. Garrett, and K.A. Peterson, J. Chem. Phys. **116**, 4142 (2002).

[23] Z. Peng, S. Kristyan, and A. Kuppermann, Phys. Rev. A **52**, 1005 (1995).

[24] U. Galster, F. Baumgartner, U. Müller, H. Helm, and M. Jungen, Phys. Rev. A **72**, 062506 (2005).

[25] R.N. Porter and M. Karplus, J. Chem. Phys. **40**, 1105 (1964).

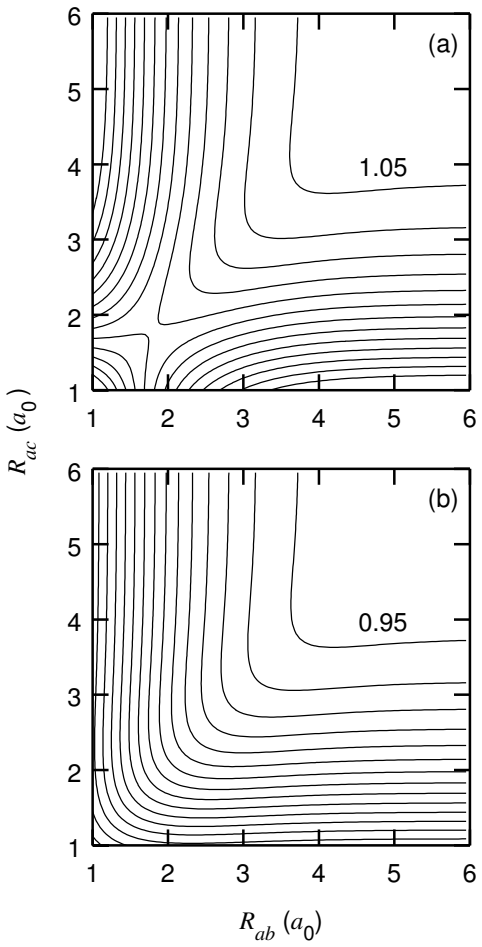

Figure 1–Constant-value contours for the two largest doublet eigenvalues of the $\mathbf{P_A}(\boldsymbol{R})$ matrix of Eq. (17) for collinear atomic configurations of H_3 constructed in a $1s^3$ representation, employing an increment/decrement of 0.05 between adjacent contours. The coordinate axes give the distances R_{ab} and R_{ac} between the central atom located at the origin and the outer atoms, measured in atomic units (a_0). In panel (a) the contours increase uniformly in value from that labeled 1.05, except as $R_{ab} = R_{ac} \rightarrow 0$ inside the saddle point, in which region the values decrease monotonically to zero, whereas in panel (b) the contour values decrease uniformly from that labeled 0.95.

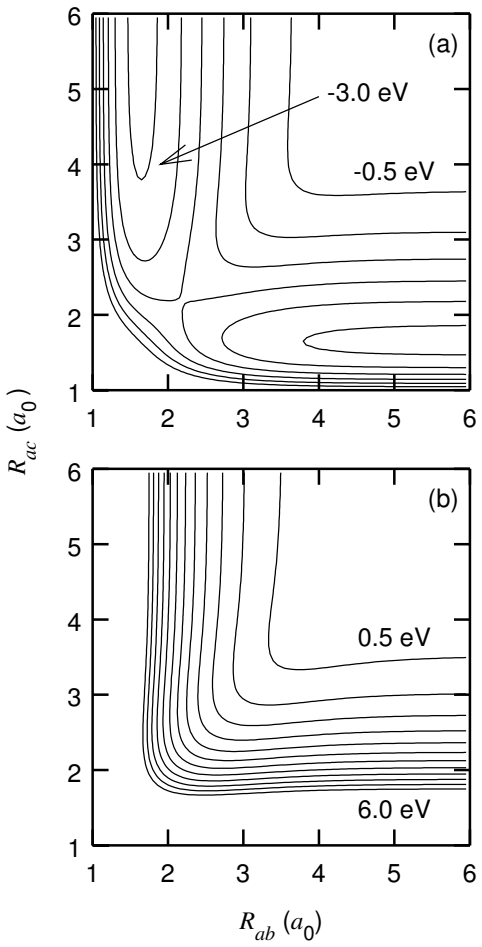

Figure 2–Constant-energy contours for the ground and first excited doublet-state potential energy surfaces of H_3 for non-symmetric collinear atomic arrangements, obtained from Eqs. (23) to (26) in a $1s^3$ representation, employing an energy decrement/increment of 0.5 eV between contours. The coordinate axes are as in Fig. 1, and the zero of energy employed (-1.50 au) is that of the three-atom dissociation limt (H+H+H). Panel (a) depicts the familiar saddle and diatomic structures of the ground-state energy surface in H_3 [25], whereas the excited-state energy surface of panel (b) is montonically increasing with decreasing separations R_{ab} and/or R_{ac}.

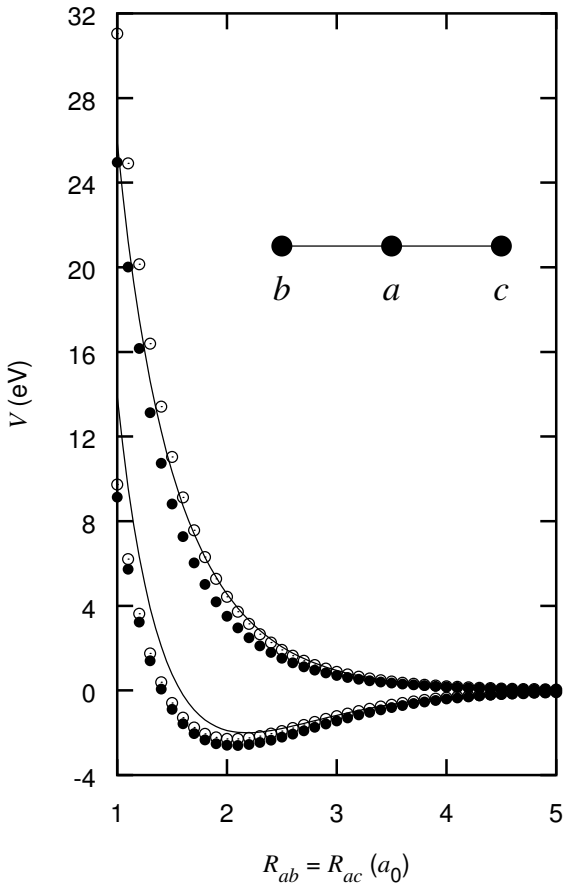

Figure 3–Ground and first-excited doublet state energies in H_3 for symmetric collinear atomic arrangements. The solid curves depict the values obtained from Eqs. (23) to (26) in a $1s^3$ representation, whereas the data points are obtained from conventional valence-bond calculations in a $1s^3$ basis set including (•) and excluding (◦) ionic configurations [20]. The zero of energy employed (-1.50 au) is that of the three-atom dissociation limit (H+H+H), as in Fig. 2.

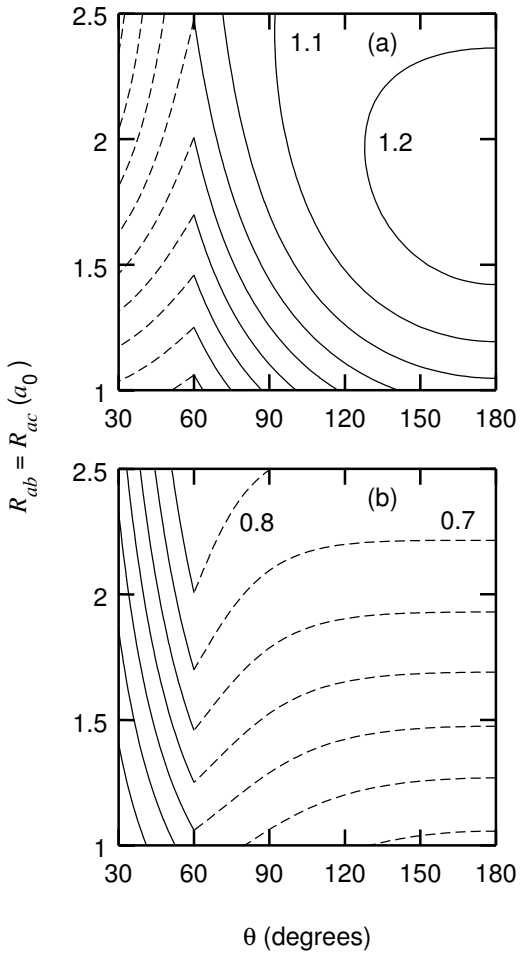

Figure 4–Constant-value contours for the two largest doublet-state eigenvalues of the $\mathbf{P_A}(\boldsymbol{R})$ matrix of Eq. (17) in a $1s^3$ representation for C_{2v} atomic arrangements ($R_{ab} = R_{ac}$), where θ is the apex angle of the triatomic H_3 configuration, employing an increment/decrement of 0.1 between adjacent contours. The cusps in the contours of both panels indicate the presence of a seam of intersection at $\theta = 60$ degrees in two continuous surfaces identified by the solid and dashed lines, with the contour values decreasing uniformly from right to left in panel (a) and decreasing uniformly from top to bottom in panel (b), as is discussed further in the text.

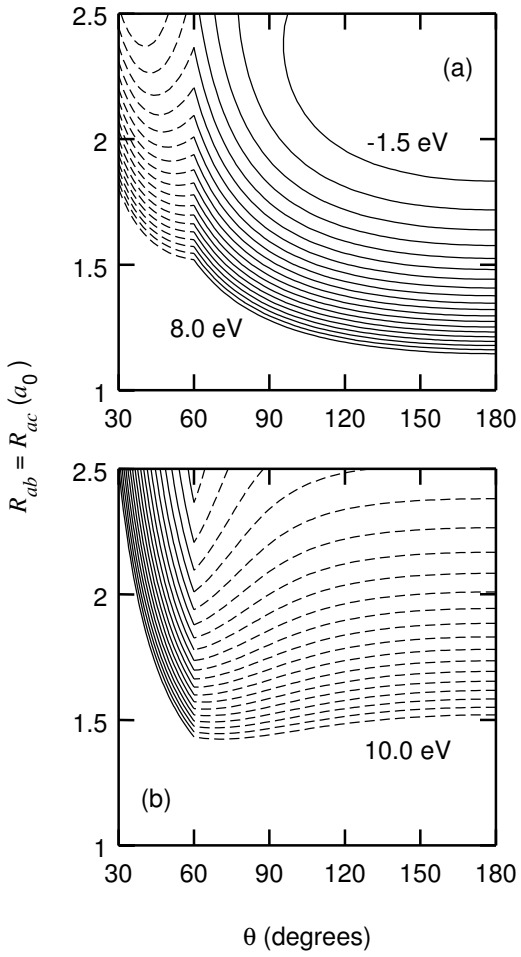

Figure 5–Constant-energy contours for the two lowest-lying doublet states of H_3 for C_{2v} atomic arrangements ($R_{ab} = R_{ac}$), obtained from Eqs. (23) to (26) in a $1s^3$ representation, where θ is the apex angle of the triatomic configuration, employing an energy increment/decrement of 0.5 eV between adjacent contours. The zero of energy (-1.50 au) is that of the three-atom dissociation limit (H+H+H). The cusps in the contours of both panels indicate the familiar D_{3h} symmetry seam of intersection at $\theta = 60$ degrees in the two continuous energy surfaces identified by the solid and dashed lines [25], with the contour energy values increasing uniformly from top to bottom in both panels. Panel (a) depicts the lowest-lying surface only for values of $\theta \geq 60$ degrees, whereas panel (b) depicts the lowest-lying surface only for $\theta \leq 60$ degrees, as is discussed further in the text.

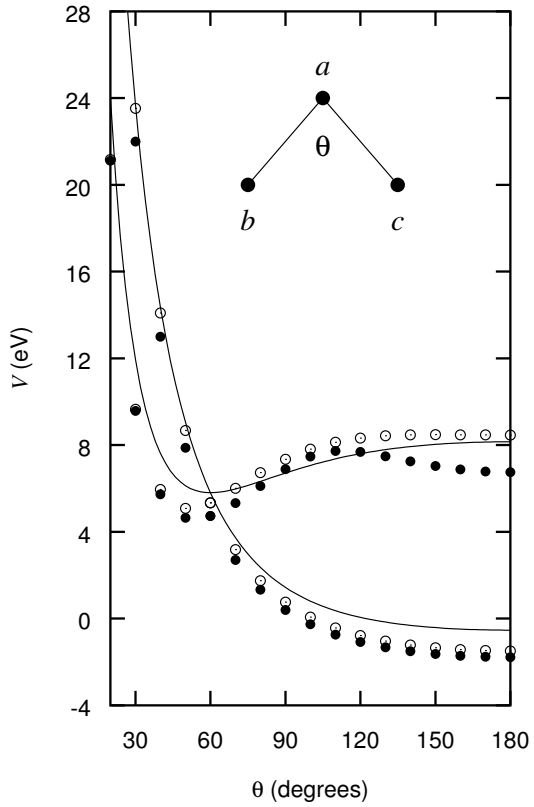

Figure 6–Ground and first-excited doublet-state energies in H_3 for C_{2v} atomic arrangements ($R_{ab} = R_{ac} = 1.64\ a_0$), where θ is the apex angle of the triatomic configuration. The solid curves depict the values obtained from Eqs. (23) to (26) in a $1s^3$ representation, whereas the data points are obtained from conventional valence-bond calculations in a $1s^3$ basis set including (•) and excluding (○) ionic configurations [20]. The zero of energy (-1.50 au) is that of the three-atom dissociation limit (H+H+H), as in Fig. 5. The crossing point of the two curves corresponds to D_{3h} symmetry, as discussed further in the text.